

## Massive neutron stars and their implications

T K JHA<sup>1,\*</sup> and KESHAB C PANDA<sup>2</sup>

<sup>1</sup>Department of Physics, BITS Pilani K K Birla Goa Campus, Goa 403 726, India

<sup>2</sup>School of Physics, Sambalpur University, Jyoti Vihar 768 019, India

\*Corresponding author. E-mail: tkjha@goa.bits-pilani.ac.in

DOI: 10.1007/s12043-014-0736-3; ePublication: 2 May 2014

**Abstract.** Recent observations of high mass pulsar PSRJ1614-2230 has raised serious debate over the possible role of exotics in the dense core of neutron stars. The precise measurement of mass of the pulsar may play a very important role in limiting equation of state (EoS) of dense matter and its composition. Indirectly, it may also shape our understanding of the nucleon–hyperon or hyperon–hyperon interactions which is not well known. Within the framework of an effective chiral model, we compute models of neutron stars and analyse the hyperon composition in them. Further related implications are also discussed.

**Keywords.** Equation of state; neutron stars; hyperons.

PACS Nos 21.65.+f; 13.75.Cs; 97.60.Jd; 21.30.Fe; 25.75.–q; 26.60.+c

### 1. Introduction

The properties of neutron stars (observed as pulsars) serve as a natural laboratory to study the dense matter interactions and compositions [1]. Observationally, it is very tough to pinpoint on the composition of dense core of these stars and therefore, one reverts to theoretical means to calculate the relevant properties of stars. In such a scenario, it becomes imperative to look for a realistic equation of state (EoS) of dense matter, which is an input to obtain models of pulsars. In this regard, the effective chiral model has been employed to study both the static and the rotating neutron stars with a hyperon core [2]. Our results very well matches with some recent observations of high mass stars [3] and has some interesting implications. Massive neutron stars are not only exotic species, but being gravitationally more bound, they can be stable to fast rotations. Observationally, currently the fastest rotating pulsar rotates at 716 Hz [4]. On the one hand, observation of massive neutron stars throws important implications to the possible role of exotics in dense core of these stars, and on the other hand such high rotations may lead to substantial deformation in the star, thereby, leading to elliptical deformation and thus, may act as potential continuous gravitational waves (CGW) emitter. In the current work, we concentrate on the

possible role of hyperons in dense matter, their interactions and the corresponding effects on the global properties of the stars. From various theoretical investigations, it is well known that hyperons form a sizable population in the dense core of neutron stars, thereby leading to a softening effect on the EoS and thus, resulting in low mass stars. However, as emphasized earlier, the observation of high mass stars does not really go well with this and therefore, it becomes even more important to zoom in onto the nucleon–hyperon or hyperon–hyperon interactions to agree with the observational limits. With respect to the EoS, one then needs to regulate the degree of softening to tune with the astrophysical observations.

## 2. Equation of state

For the present work, we employ an effective chiral model to construct models of rotating neutron stars. The model and its attributes were worked out in detail in [2]. For the sake of completeness, we, however, put down the relevant thermodynamic quantities for the many-baryon system. The effective Lagrangian of the model interacting through the exchange of the pseudoscalar meson  $\pi$ , the scalar meson  $\sigma$ , the vector meson  $\omega$  and the isovector  $\rho$ -meson is given by

$$\begin{aligned} \mathcal{L} = & \bar{\psi}_B \left[ \left( i\gamma_\mu \partial^\mu - g_\omega \gamma_\mu \omega^\mu - \frac{1}{2} g_\rho \vec{\rho}_\mu \cdot \vec{\tau} \gamma^\mu \right) - g_\sigma (\sigma + i\gamma_5 \vec{\tau} \cdot \vec{\pi}) \right] \psi_B \\ & + \frac{1}{2} (\partial_\mu \vec{\pi} \cdot \partial^\mu \vec{\pi} + \partial_\mu \sigma \partial^\mu \sigma) - \frac{\lambda}{4} (x^2 - x_0^2)^2 - \frac{\lambda b}{6m^2} (x^2 - x_0^2)^3 \\ & - \frac{\lambda c}{8m^4} (x^2 - x_0^2)^4 - \frac{1}{4} F_{\mu\nu} F_{\mu\nu} + \frac{1}{2} g_{\omega B}^2 x^2 \omega_\mu \omega^\mu \\ & - \frac{1}{4} \vec{R}_{\mu\nu} \cdot \vec{R}^{\mu\nu} + \frac{1}{2} m_\rho^2 \vec{\rho}_\mu \cdot \vec{\rho}^\mu . \end{aligned} \quad (1)$$

The first line of the above Lagrangian represents the interaction of the nucleon isospin doublet  $\psi_B$  with the aforesaid mesons. In the second line we have the kinetic and the non-linear terms in the pseudoscalar–isovector pion field  $\vec{\pi}$ , the scalar field  $\sigma$  and higher-order terms of the scalar field in terms of the invariant combination of the two, i.e.,  $x^2 = \vec{\pi}^2 + \sigma^2$ . Subsequently, we have the field strength and mass term for the vector field  $\omega$  and the isovector field  $\vec{\rho}$  meson.  $g_\sigma$ ,  $g_\omega$  and  $g_\rho$  are the usual meson–nucleon coupling strength of the scalar, vector and the isovector fields, respectively. Here, we shall be concerned only with the normal non-pion condensed state of matter, so we take  $\langle \vec{\pi} \rangle = 0$  and also  $m_\pi = 0$ .

The interaction of the scalar and the pseudoscalar mesons with the vector boson generates a dynamical mass for vector bosons through spontaneous breaking of the chiral symmetry with scalar field attaining the vacuum expectation value  $x_0$ . Then, the mass of the nucleon ( $m$ ), the scalar ( $m_\sigma$ ) and the vector meson ( $m_\omega$ ), are related to  $x_0$  through

$$m = g_\sigma x_0, \quad m_\sigma = \sqrt{2\lambda} x_0, \quad m_\omega = g_\omega x_0 . \quad (2)$$

To obtain the EoS, we revert to the mean-field procedure in which, one assumes the mesonic fields to be uniform, i.e., without any quantum fluctuations. The vector field ( $\omega$ ),

the scalar field ( $\sigma$ ) (in terms of  $Y = x/x_0 = m^*/m$ ) and the isovector field ( $\rho$ ) are, respectively given by

$$\omega_0 = \sum_B \frac{\rho_B}{g_\omega x^2}, \quad (3)$$

$$(1 - Y^2) - \frac{b}{m^2 c_\omega} (1 - Y^2)^2 + \frac{c}{m^4 c_\omega^2} (1 - Y^2)^3 + \frac{2c_\sigma c_\omega \rho_B^2}{m^2 Y^4} - \frac{2c_\sigma \rho_S}{mY} = 0 \quad (4)$$

$$\rho_{03} = \sum_B \frac{g_\rho}{m_\rho^2} I_3 \rho_B. \quad (5)$$

The quantity  $\rho_B$  and  $\rho_S$  are the vector and the scalar densities,  $k_F$  is the Fermi momentum of the baryon and  $\gamma = 4$  (symmetric matter) is the spin degeneracy factor. The total energy density  $\varepsilon$  and pressure  $P$  of the symmetric nuclear matter for a given baryon density is

$$\begin{aligned} \varepsilon = & \frac{\gamma}{2\pi^2} \int_0^{k_F} k^2 dk \sqrt{k^2 + m^{*2}} + \frac{m^2(1 - Y^2)^2}{8c_\sigma} - \frac{b}{12c_\omega c_\sigma} (1 - Y^2)^3 \\ & + \frac{c}{16m^2 c_\omega^2 c_\sigma} (1 - Y^2)^4 + \frac{c_\omega \rho_B^2}{2Y^2}, \end{aligned} \quad (6)$$

$$\begin{aligned} P = & \frac{\gamma}{6\pi^2} \int_0^{k_F} \frac{k^4 dk}{\sqrt{k^2 + m^{*2}}} - \frac{m^2(1 - Y^2)^2}{8c_\sigma} + \frac{b}{12c_\omega c_\sigma} (1 - Y^2)^3 \\ & - \frac{c}{16m^2 c_\omega^2 c_\sigma} (1 - Y^2)^4 + \frac{c_\omega \rho_B^2}{2Y^2}. \end{aligned} \quad (7)$$

The meson field equations for  $\omega$  (eq. (3)) and  $\sigma$ -meson (eq. (4)) are solved self-consistently at a fixed baryon density to obtain the respective field strengths and the corresponding energy density and pressure are calculated.

For calculating the EoS of neutron star matter, we included the octet of baryons by generalizing the Lagrangian. For a detailed derivation within the framework, one may refer to [2]. The equations for the structure of a relativistic spherical and static star composed of a perfect fluid were derived from Einstein's equations by Tolman, Oppenheimer and Volkoff [5], which are

$$\frac{dP}{dr} = -\frac{G}{r} \frac{[\varepsilon + P][M + 4\pi r^3 P]}{(r - 2GM)}, \quad (8)$$

$$\frac{dM}{dr} = 4\pi r^2 \varepsilon, \quad (9)$$

with  $G$  as the gravitational constant and  $M(r)$  as the enclosed gravitational mass. We have used  $c = 1$ . Given an EoS, these equations can be integrated from the origin as an initial value problem for a given choice of central energy density,  $\varepsilon_c$ . The value of  $r$  ( $=R$ ), where the pressure vanishes, defines the surface of the star. We solve the above equations to study the structural properties of a static neutron star using the EoS derived for the electrically charged neutral hyperonic dense matter [6,7].

### 3. Results and discussion

In the present calculations, we take the selected parameters of the model [8], that satisfy nuclear matter saturation properties at density ( $\rho_0 = 0.153 \text{ fm}^{-3}$ ), which agrees with the observed charge and mass distribution of the finite nuclei. The binding energy per nucleon is fixed at the empirical value  $B/A - m = -16.3 \text{ MeV}$  [1]. The selected parameters are enlisted in table 1. The two models considered here (SI and SII) have been chosen to differ in nuclear incompressibility. SI represents a stiff EoS ( $K = 303 \text{ MeV}$ ) and SII represents a soft EoS with  $K = 231 \text{ MeV}$ . The nucleon effective mass is consistent with the results from the analysis of neutron scattering of lead nuclei [1] with the range  $m^*/m = (0.80-0.90)$ . It is known that a lower nucleon effective mass is known to reproduce the finite nuclei properties, such as the spin-orbit effects splitting correctly [9].

Selected models for further studies are employed to extract the relevant thermodynamic quantities. The resulting binding energy per nucleon for symmetric nuclear matter (SNM) and pure neutron matter (PNM) for the two models is plotted in figure 1a. The difference in the two models (particularly in the incompressibility values) is very well reflected in the plot. In comparison to the successful mean-field models (say NL3), nuclear matter saturates at a density slightly lower ( $\rho_0 = 0.148 \text{ fm}^{-3}$ ) than what we have taken in the present calculation, and the binding energy per nucleon remains almost same ( $\approx -16.3 \text{ MeV}$ ). In the case of DBHF, nuclear matter saturates at still higher density. It is worth noticing that, the incompressibility of the present model spans within 230–303 MeV in comparison to that predicted by the NL3 parameter set which has  $K = 271.6 \text{ MeV}$ . Incompressibility of nuclear matter is the measure of the degree of softness/stiffness of the EoS. Conventionally, EoS with  $K < 300 \text{ MeV}$  are considered to be soft. It should be interesting to study the consequences of such behaviour in the astrophysical context, especially on the global properties and structure of neutron stars at physically interesting densities ( $2-5\rho_0$ ) [11,12].

In figure 1b, the nucleon effective mass in the nuclear medium is plotted as a function of baryon density up to  $4\rho_0$ . This medium mass modification of nucleon in nuclear medium is a consequence of the Dirac field and forms an essential element for the success of

**Table 1.** Selected parameter sets of the effective chiral model employed in the present work. The binding energy per nucleon is  $B/A - m = -16.3 \text{ MeV}$  and the asymmetry energy coefficient  $J \approx 32 \text{ MeV}$  at saturation density  $\rho_0 = 0.153 \text{ fm}^{-3}$ . The nucleon, the vector meson and the isovector vector meson masses are taken to be 939, 783 and 770 MeV, respectively and  $c_\sigma = (g_\sigma/m_\sigma)^2$ ,  $c_\omega = (g_\omega/m_\omega)^2$  and  $c_\rho = (g_\rho/m_\rho)^2$  are the corresponding coupling constants.  $B = b/m^2$  and  $C = c/m^4$  are the higher-order constants in the scalar field. Other derived quantities such as the scalar meson mass  $m_\sigma$ , the pion decay constant  $f_\pi$  and the nuclear matter incompressibility,  $K$ , at  $\rho_0$  are also given (adapted from [8]).

Model	$c_\sigma$ (fm <sup>2</sup> )	$c_\omega$ (fm <sup>2</sup> )	$c_\rho$ (fm <sup>2</sup> )	$B$ (fm <sup>2</sup> )	$C$ (fm <sup>4</sup> )	$m_\sigma$ (MeV)	$Y$	$f_\pi$ (MeV)	$K$ (MeV)
SI	6.77	1.99	5.29	-4.27	0.29	510	0.85	140	303
SII	7.33	1.64	5.32	-6.59	0.57	445	0.87	154	231

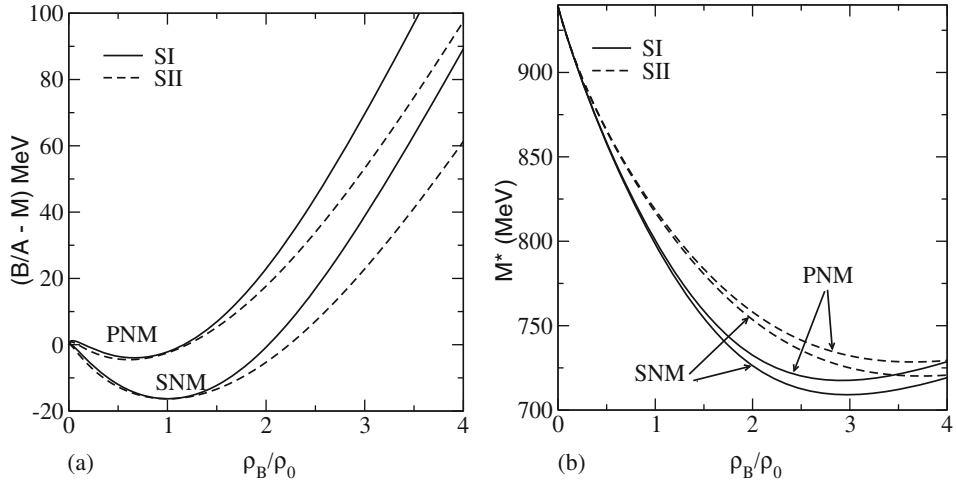


**Figure 1.** (a) Binding energy per nucleon as a function of normalized baryon density for the pure neutron matter (PNM,  $\gamma = 2$ ) and symmetric nuclear matter (SNM,  $\gamma = 4$ ) for the selected models given in table 1. (b) Nucleon effective mass is plotted as a function of normalized baryon density for the pure neutron matter (PNM) and symmetric nuclear matter (SNM) cases for the two models.

the relativistic phenomenology. From the plot, it is interesting to see that the nucleon experiences repulsive forces in nuclear matter at higher densities ( $\rho_B > 2\rho_0$ ), as a result of which the nucleon effective mass increases again for the three cases that we study at present. At saturation density, the present model results in much higher nucleon effective mass in comparison to the NL3 ( $m^*/m = 0.60$ ) and DBHF ( $m^*/m = 0.678$ ).

The models are then employed to study the neutron star properties. The energy density and the pressure are calculated for a hyperon-rich neutron star matter, which is then subjected to the hydrodynamic equilibrium, results in star properties such as mass and radius for the particular equation of state. To analyse the hyperon-rich matter, we include the octet of baryons in the core of these stars and calculate both the static as well as rotating neutron star models. We use the code written by Stergioulas [10] based on the Komatsu–Eriguchi–Hachisu method to construct uniformly rotating star models in the axis-symmetric basis.

The composition of charge neutral dense matter is very sensitive to the hyperon–meson coupling parameters which however, are very poorly known [11,12]. There are different phenomenological prescriptions e.g., using the quark counting arguments based on  $SU(6)$  theory to fix the vector couplings, while, fixing the scalar couplings from the potential depths of hyperon in nuclear matter [13–15]. From various analyses the choice of the ratio of hyperon to nucleon coupling for  $\sigma$  meson  $x_\sigma < 0.72$  has been emphasized [16] and also from studies based on hypernuclear levels, the choice ( $x_\sigma < 0.9$ ) is bounded from above. ‘From above’ signifies the maximum scalar meson coupling to the hyperon with respect to the nucleon, which is obtained from hypernuclei experiments. Following this convention, in this work we take  $x_\sigma = g_{\sigma H}/g_{\sigma N} = 0.8$ ,  $x_\omega = g_{\omega H}/g_{\omega N} = 0.85$  and  $x_\omega = x_\rho$ , to calculate the EoS for the neutron star matter for both the models SI and SII.

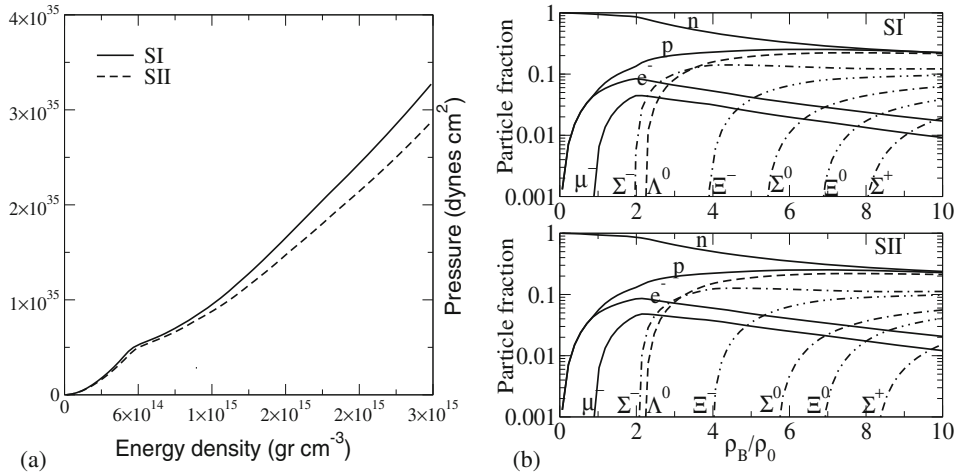


**Figure 2.** (a) Pressure of the neutron star matter (including the octet of baryons) is plotted as a function of energy density of the system upto nearly  $10\rho_0$ . (b) Particle fraction of the octet of baryons ( $n$ ,  $p$ ,  $\Lambda^0$ ,  $\Sigma^{-,0,+}$ ,  $\Xi^{-,0}$ ) and leptons ( $e^-$ ,  $\mu^-$ ) in the neutron star matter for the two models considered here.

The resulting EoS of hyperon-rich matter is displayed in figure 2a and the corresponding particle population in figure 2b. Here, it can be seen that SI and SII accommodate all the octet of baryons upto ten times the normal nuclear matter density although the hyperons start appearing at higher densities in the latter case. In general, the hyperons start appearing at  $\approx 2\rho_0$  and are the dominant species on par with nucleons at  $\approx 10\rho_0$ . It can also be seen that the negatively charged particle species are favoured in the dense matter composition followed by the neutral ones and the positively charged counterparts. For example, in all the three cases, one finds that  $\Sigma^-$  appears before  $\Lambda^0$  although the vacuum mass difference between the two is  $\approx 77$  MeV and the former is more massive than the latter. This is due to the fact that as the density is increased ( $\approx 2\rho_0$ ), the negatively-charged  $\Sigma^-$  starts competing with the negatively-charged leptons in maintaining charge neutrality of the dense matter. Due to the depletion of the lepton concentration, the corresponding chemical potential  $\mu_e$  decreases, thereby lowering the threshold chemical potential of  $\Sigma^-$  as compared to  $\Lambda^0$ . Similar arguments exist for the other negatively-charged baryons.

Although a relativistic compact star has much complicated internal structure, its properties can be reasonably approximated by some simplifying assumptions. The matter inside is assumed to be a perfect fluid on the basis of the observation from pulsar glitches, which shows that the departure from perfect fluid equilibrium due to the solid crust is quite negligible ( $\sim 10^{-5}$ ) [17]. At birth, a neutron star is differentially rotating, but because of several factors such as the cooling phenomenon, shear viscosity, neutrino diffusion etc., the star assumes a uniform rotation. So, the approximation of a zero temperature perfect fluid neutron star matter is a good one. The properties of the neutron star is unique to the EoS considered. Using these EoS we now calculate some of the global properties of the neutron star, which is rotating at its Kepler velocity ( $\Omega_K$ ) by employing the RNS (rotating neutron star) code [10].

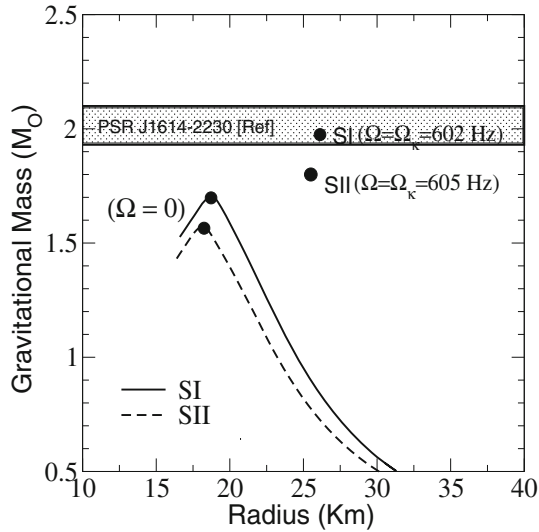


**Figure 3.** Mass–radius relationship plotted for the models considered for the static as well as them rotating at Kepler frequency. The mass limit for PSR J1614-2230 ( $1.97 \pm 0.04 M_{\odot}$ ) is plotted for reference. The Kepler frequencies obtained for models SI and SII are 602 and 605 Hz, respectively.

In general, rotation stabilizes the star against gravitational collapse and therefore, rotating neutron stars are more massive than the static ones. Further, the additional centrifugal forces in a rotating star help to counteract the pull of gravity, resulting in larger radii for a given mass. In figure 3, we plot the mass of the neutron star as a function of radius for both the static as well as them rotating at Kepler frequency. In order to evaluate the radius of the star, we have included the BPS EoS [18] at subnuclear densities which contributes to the crustal part of the star structure. The radius obtained for the EoS lies in the range 25–26 km. It is to be noted that the large radius obtained in the rotating case corresponds to the equatorial radius of the star, because of the centrifugal forces that act on the star owing to the high rotations which are absent in the case of static star. From the

**Table 2.** Global properties of the star in both the static limit ( $\Omega = 0$ ) in the first row and the corresponding models rotating at Kepler frequency ( $\Omega = \Omega_K$ ) in the second row for the models SI and SII as given in table 1.  $M_G$  is the gravitational mass,  $M_B$  is the baryonic mass and  $\epsilon_c$  is the central density of the star. Radius, moment of inertia  $I$ , quadruple moment  $\phi_{22}$  and the rotational frequency  $f$  are also given.

Model	$M_G$ ( $M_{\odot}$ )	$\epsilon_c$ ( $10^{14} \text{ g cm}^{-3}$ )	$M_B$ ( $M_{\odot}$ )	Radius (km)	$I$ ( $10^{45} \text{ g cm}^2$ )	$\phi_{22}$ ( $10^{42} \text{ g cm}^2$ )	$f$ (Hz)
SI	1.70	8.15	1.80	18.73	–	–	–
	1.96	7.53	2.10	26.20	4.875	5.365	602
SII	1.57	8.00	1.66	16.60	–	–	–
	1.80	8.00	1.90	25.50	4.068	4.468	605

observational point of view, there are large uncertainties in the determination of radius of the star [19–21], primarily due to a lack of knowledge of the composition of star atmosphere, large distance and also due to the presence of high magnetic fields. On the other hand, the general relativistic limit for the compactness parameter assuming a uniform density star with the causal EoS i.e.,  $P = \varepsilon$  gives  $M/R < 4/9$  [1]. Here, we have shown the observational limit for the recent discovery of pulsar PSRJ1614-2230 with a mass of  $1.97 \pm 0.04 M_{\odot}$ . We find that rotating stars do agree with the observational data.

The overall results for the global properties of the star are summarized in table 2.

#### 4. Conclusion

In the present work, we study the rotational attributes of the neutron stars in a relativistic framework in the mean-field approach using an effective chiral hadronic model generalized to include all the octets of baryons. The EoS employed differ in incompressibility, which we compare with regard to the neutron star properties. From this analysis, it is conclusive that hyperons form a sizeable population in the dense matter and with higher nucleon effective mass, the threshold for the appearance of the respective hyperon species is pushed further to the higher densities. Hyperons are found to have a substantial impact on the density region relevant to neutron star properties and are known to decrease the maximum mass of the star. The ongoing and future experimental hypernuclear programmes such as those at Jefferson Lab, KEK, J-PARC and GSI, Darmstadt, FAIR etc., will provide decisive insights into the role of these exotic forms of matter in dense matter EoS and hence neutron stars, so as to efficiently constrain the dense matter EoS.

We have calculated the global properties of rotating neutron star sequences such as the mass, radius, central density, moment of inertia and Kepler angular velocity in the KEH method or the fast rotation approach. The maximum mass obtained at Keplerian velocity for the models lies in the range  $1.8\text{--}2.0 M_{\odot}$  which is in very good agreement with the recent observations of massive neutron stars such as PSRJ1614-2230 [3], although we do find substantial increase in the star radius. The corresponding central density at maximum mass is nearly in the range  $3.0\rho_0$ . Subsequently, the circumferential radii obtained for the cases lie in the range 25–26 km. Further, we have obtained the Kepler frequency of  $\nu = 600$  Hz for both the models SI and SII.

The observation of high mass stars has raised considerable amount of debate over the nature of EoS, i.e., the stiffness or softness of the EoS at high densities. Besides, the analysis in the present work throws interesting insights with regard to the implications of heavy-ion collision data on the neutron star structure. The present EoS results in small Kepler frequency and larger equatorial radius, which is because of the softening of the EoS at higher densities. However, we would like to mention here that more systematic calculations are required before we arrive at some precise conclusions on the constraints of dense matter EoS and neutron star properties provided by the present model. We have explored here the model of a neutron star with a hyperon core. It will be interesting to study and analyse these results including the phase transition aspects such as the transition to superconducting quark matter in the neutron star core, which we shall take up in our next endeavour.



## Acknowledgement

One of the authors, TKJ, would like to thank BRNS for the support for the work [2013/37P/5/BRNS].

## References

- [1] S L Shapiro and S A Teukolski, *Black holes, white dwarfs, and neutron stars* (Wiley, New York, 1983)  
N K Glendenning, *Compact stars: nuclear physics, particle physics, and general relativity* (Springer Verlag, 2000)
- [2] P K Sahu and A Ohnishi, *Prog. Theor. Phys.* **104**, 1163 (2000)  
P K Sahu, T K Jha, K C Panda and S K Patra, *Nucl. Phys. A* **733**, 169 (2004)  
T K Jha, P K Raina, P K Panda and S K Patra, *Phys. Rev. C* **75**, 029903(E) (2007)  
T K Jha, P K Raina, P K Panda and S K Patra, *Phys. Rev. C* **74**, 055803 (2006)  
T K Jha, H Mishra and V Sreekanth, *Phys. Rev. C* **77**, 045801 (2008)
- [3] P B Demorest, T Pennucci, S M Ransom, M S E Roberts and J W T Hessels, *Nature* **467**, 1081 (2010)
- [4] J W T Hessels *et al*, *Science* **311**, 1901 (2006)
- [5] J R Oppenheimer and G M Volkoff, *Phys. Rev.* **55**, 374 (1939)  
R C Tolman, *Phys. Rev.* **55**, 364 (1939)
- [6] J M Lattimer and M Prakash, *Phys. Rep.* **333**, 121 (2000)  
J M Lattimer and M Prakash, *Science* **304**, 536 (2004)
- [7] P G Krastev and F Sammarruca, *Phys. Rev. C* **74**, 025808 (2006)  
H Heiselberg and V Pandharipande, *Ann. Rev. Nucl. Part. Sci.* **50**, 481 (2000)
- [8] T K Jha and H Mishra, *Phys. Rev. C* **78**, 065802 (2008)
- [9] R J Furnstahl, J J Rusnak and B D Serot, *Nucl. Phys. A* **632**, 607 (1998)
- [10] N Stergioulas and J L Friedman, *Astrophys. J.* **444**, 306 (1995)
- [11] M Prakash, I Bombaci, M Prakash, P J Ellis, J M Lattimer and R Knorren, *Phys. Rep.* **280**, 1 (1997)
- [12] N K Glendenning, *Phys. Lett. B* **114**, 392 (1982); *Astrophys. J.* **293**, 470 (1985); *Z. Phys. A* **326**, 57 (1987)
- [13] J Schaffner-Beilich and I N Mishustin, *Phys. Rev. C* **53**, 1416 (1996)
- [14] A Mishra, P K Panda and W Greiner, *J. Phys. G* **28**, 67 (2002)
- [15] J Schaffner, C B Dover, A Gal, D J Millener, C Greiner and H Stöcker, *Ann. Phys. (N.Y.)* **235**, 35 (1994)  
S Banik and D Bandyopadhyay, *Phys. Rev. C* **63**, 035802 (2001)  
C B Dover, D J Miller and A Gal, *Phys. Rep.* **184**, 1 (1989)
- [16] N K Glendenning and S A Moszkowski, *Phys. Rev. Lett.* **67**, 2414 (1991)
- [17] J L Friedman and J R Ipser, *Philos. Trans. R. Soc. London A* **340**, 391 (1992)
- [18] G Baym, C Pethick and P Sutherland, *Astrophys. J.* **170**, 299 (1971)
- [19] R Rutledge, L Bildsten, E Brown, G Paplov and V Zavlin, *Astrophys. J.* **577**, 346 (2002); *Astrophys. J.* **578**, 405 (2002)
- [20] B Gendre, D Barret and N A Webb, *Astron. Astrophys.* **400**, 521 (2003)  
W Becker *et al*, *Astrophys. J.* **594**, 364 (2003)
- [21] J Cottam, F Paerels and M Mendez, *Nature* **420**, 51 (2002)